Evaluation of bone remodeling around single dental implants of different lengths: a mechanobiological numerical simulation and validation using clinical data

ARTICLE *in* COMPUTER METHODS IN BIOMECHANICS AND BIOMEDICAL ENGINEERING · AUGUST 2015

Impact Factor: 1.77 · DOI: 10.1080/10255842.2015.1052418 · Source: PubMed

6 AUTHORS, INCLUDING:

Bruno Salles Sotto Maior

Federal University of Juiz de Fora

44 PUBLICATIONS **95** CITATIONS

SEE PROFILE

Emílio Mercuri

Universidade Federal do Paraná

10 PUBLICATIONS **3** CITATIONS

SEE PROFILE

Plinio Mendes Senna

Universidade do Grande Rio (UNIGRANRIO)

40 PUBLICATIONS **110** CITATIONS

SEE PROFILE

Altair A Del Bel Cury

University of Campinas

248 PUBLICATIONS **2,421** CITATIONS

SEE PROFILE

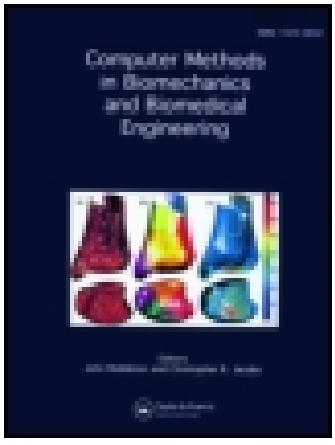

Computer Methods in Biomechanics and Biomedical Engineering

Publication details, including instructions for authors and subscription information:
http://www.tandfonline.com/loi/gcmb20

Evaluation of bone remodeling around single dental implants of different lengths: a mechanobiological numerical simulation and validation using clinical data

Bruno Salles Sotto-Maior[a], Emílio Graciliano Ferreira Mercuri[b], Plinio Mendes Senna[c], Neuza Maria Souza Picorelli Assis[a], Carlos Eduardo Francischone[d] & Altair Antoninha Del Bel Cury[e]

[a] Department of Restorative Dentistry, Federal University of Juiz de Fora, Juiz de Fora, Brazil

[b] Department of Environmental Engineering, Federal University of Paraná, Curitiba, Brazil

[c] Department of Health Sciences Center, Unigranrio University, Duque de Caxias, Rio de Janeiro, Brazil

[d] Department of Implantology, São Leopoldo Mandic Institute and Research Center, Campinas, Brazil

[e] Department of Prosthodontic and Periodontology, Piracicaba Dental School, Campinas State University, Campinas, Brazil

Published online: 07 Aug 2015.

To cite this article: Bruno Salles Sotto-Maior, Emílio Graciliano Ferreira Mercuri, Plinio Mendes Senna, Neuza Maria Souza Picorelli Assis, Carlos Eduardo Francischone & Altair Antoninha Del Bel Cury (2015): Evaluation of bone remodeling around single dental implants of different lengths: a mechanobiological numerical simulation and validation using clinical data, Computer Methods in Biomechanics and Biomedical Engineering, DOI: 10.1080/10255842.2015.1052418

To link to this article: http://dx.doi.org/10.1080/10255842.2015.1052418

Computer Methods in Biomechanics and Biomedical Engineering, 2015
http://dx.doi.org/10.1080/10255842.2015.1052418

Taylor & Francis
Taylor & Francis Group

Evaluation of bone remodeling around single dental implants of different lengths: a mechanobiological numerical simulation and validation using clinical data

Bruno Salles Sotto-Maior[a]*, Emílio Graciliano Ferreira Mercuri[b], Plinio Mendes Senna[c], Neuza Maria Souza Picorelli Assis[a], Carlos Eduardo Francischone[d] and Altair Antoninha Del Bel Cury[e]

[a]*Department of Restorative Dentistry, Federal University of Juiz de Fora, Juiz de Fora, Brazil;* [b]*Department of Environmental Engineering, Federal University of Paraná, Curitiba, Brazil;* [c]*Department of Health Sciences Center, Unigranrio University, Duque de Caxias, Rio de Janeiro, Brazil;* [d]*Department of Implantology, São Leopoldo Mandic Institute and Research Center, Campinas, Brazil;* [e]*Department of Prosthodontic and Periodontology, Piracicaba Dental School, Campinas State University, Campinas, Brazil*

(*Received 23 March 2014; accepted 14 May 2015*)

Algorithmic models have been proposed to explain adaptive behavior of bone to loading; however, these models have not been applied to explain the biomechanics of short dental implants. Purpose of present study was to simulate bone remodeling around single implants of different lengths using mechanoregulatory tissue differentiation model derived from the Stanford theory, using finite elements analysis (FEA) and to validate the theoretical prediction with the clinical findings of crestal bone loss. Loading cycles were applied on 7-, 10-, or 13-mm-long dental implants to simulate daily mastication and bone remodeling was assessed by changes in the strain energy density of bone after a 3, 6, and 12 months of function. Moreover, clinical findings of marginal bone loss in 45 patients rehabilitated with same implant designs used in the simulation ($n = 15$) were computed to validate the theoretical results. FEA analysis showed that although the bone density values reduced over time in the cortical bone for all groups, bone remodeling was independent of implant length. Clinical data showed a similar pattern of bone resorption compared with the data generated from mathematical analyses, independent of implant length. The results of this study showed that the mechanoregulatory tissue model could be employed in monitoring the morphological changes in bone that is subjected to biomechanical loads. In addition, the implant length did not influence the bone remodeling around single dental implants during the first year of loading.

Keywords: bone remodeling; mechanobiological; dental implants

Introduction

Bone is a tissue subjected to continuous cycles of resorption and new bone formation, known as remodeling process. It is regulated by groups of osteoclasts and osteoblasts organized into basic multicellular units that determine bone mass and its microarchitecture (McNamara & Prendergast 2007; Chou & Müftü 2013; Wazen et al. 2013). Despite physiological, biological, anatomical, and inflammatory factors that influence bone remodeling, investigations have been performed to recognize the biomechanical conditions that influence its regeneration as a nonphysiological remodeling phenomenon (Qian et al. 2012; Froum et al. 2013; Monje et al. 2014; Hof et al. 2015).

The role of biomechanical stimuli as a functional factor affecting the bone remodeling process was first described by Wolff in 1986, who observed a relationship between the internal architecture of bone and the loading direction (Wolff's Law). Moreover, other experimental studies showed that the mechanical strain is a key parameter for bone remodeling (Stanford & Brand 1999; Frost 2003), in which the physiological strain values can lead to bone formation while extreme low or high strains can cause bone resorption (Huiskes 2000; Frost 2003; Mellal et al. 2004; Gong et al. 2010; Shunmugasamy et al. 2010; Schulte et al. 2011; Chou & Müftü 2013; Eser et al. 2013; Mahnama et al. 2013). However, the bone strain threshold that leads to a physiological remodeling has not been fully established.

In dental implantology, the success of implant-supported prostheses as a replacement for missing teeth depends on adequate bone support to allow the distribution of the masticatory forces to the tissues (Brånemark et al. 1969). The stress and strain concentrated at the crestal cortical bone around the implants results in structural and morphological changes especially during the first year after the prosthetic loading (Jung et al. 1996).

However, the bone availability at the posterior regions of the jaws is usually limited, demanding the use of short implants to support the dental prostheses. Although short implants can be an alternative to rehabilitate resorbed ridges, the smaller contacting area with bone can lead to stress and strain concentration in the

*Corresponding author. Email: bruno.sotto@ufjf.edu.br

bone and affect the remodeling process (Adell 1983). This higher stress and strain can cause extensive bone remodeling (Adell 1983), but it is unknown whether it can be considered a risk for the success of osseointegration.

It is not easy to determine the strain threshold in which bone resorption stops and new bone formation starts in the remodeling process by clinical data since several bias are commonly present and not easily controlled in dental studies, such as local bone density, masticatory forces, and patients' diet. Thus, predicting this remodeling process as a function of mechanical loading is not simple through clinical experiments. In this way, mathematical models have been developed to investigate the mechanoregulatory processes of bone and help understanding the remodeling process (McNamara & Prendergast 2007; Wang et al. 2013).

On the basis of these mathematical studies, the mechanoregulatory tissue differentiation model was developed by Jacobs in 1995, which mathematically predicted changes in bone morphology and density on the basis of various mechanical stimuli such as strain, stress, or strain energy density in accordance with 'Wolff's Law' (Levenston et al. 1994). Although this model has been applied on dental implants to check the influence of prosthesis cantilever on bone remodeling (Wang et al. 2013), it is unknown if this model is sensitive enough to preview the bone remodeling around single dental implants with different lengths.

Therefore, the aim of the present study was (a) to simulate the bone remodeling around dental implants of different lengths by mechanoregulatory tissue differentiation model using three-dimensional finite element analysis (3D FEA); and (b) to validate the theoretical prediction with the clinical findings of crestal bone loss around single dental implants after one-year follow-up.

Materials and methods

Mechanoregulatory tissue differentiation model

The mathematical model for the simulation of bone remodeling around single dental implants was constructed from the Isotropic Stanford Model. This model was originally proposed by Jacobs in 1995 (Jacobs et al. 1995), which defined the daily stress stimulus (ψ_t) as a consequence of the magnitude of the daily loading. Considering only one load type in a daily basis, the stimulus can be written as

$$\psi_t = n^{1/m}\bar{\sigma}_t; \tag{1}$$

in which n is the number of daily cycles of one load type, which was assumed as 120 cycles in the present study (Woda et al. 2006); m is an empirical constant, assumed to be equal to 4 (Eser et al. 2013); and $\bar{\sigma}_t$ is the continuum level effectively experienced by the tissue, which is defined as

$$\bar{\sigma}_t = \sqrt{2EU}; \tag{2}$$

in which E is the continuum elastic modulus; and U is the continuum strain energy density of bone. The initial elastic modulus for cortical and trabecular bones were 14.95 and 1.14 GPa, respectively, and Poisson's ratio was 0.3 and 0.26, respectively (Cruz et al. 2009). The dental implant was made of titanium, which had an elastic modulus of 110 GPa and a Poisson's ratio of 0.3 (Dittmer et al. 2010).

After t loading cycles under physiological load conditions, the daily stress stimulus (ψ_t) does not cause bone remodeling (homeostatic condition), so its value remains in an equilibrium range. The homeostatic stress (ψ_{eq}) is limited by a dead threshold (w) where neither resorption nor apposition occurs ($\psi_{eq} - w \le \psi_t \le \psi_{eq} + w$). However, when there is an underload or overload, an apposition or resorption process will take place. When the stimulus is higher than the overload stimulus ($\psi_t > \psi_{crit}$), it is expected to occur microdamage in bone followed by a resorption process (McNamara & Prendergast 2007), so the authors proposed a modification of the isotropic model, by adding fourth term in equation of the remodeling rate. This phenomenological law can be expressed as

$$\dot{r} = \begin{cases} c_1\left[\left(\psi_t - \psi_{eq}\right) + w\right] & \text{if } \left(\psi_t - \psi_{eq}\right) < -w \\ 0 \quad \text{if } -w \le \left(\psi_t - \psi_{eq}\right) \le +w \\ c_2\left[\left(\psi_t - \psi_{eq}\right) - w\right] & \text{if } \left(\psi_t - \psi_{eq}\right) > +w \text{ and } (\psi_t - \psi_{crit}) < 0 \\ -c_3\left[(\psi_t - \psi_{crit}) + z\right] & \text{if } (\psi_t - \psi_{crit}) > 0 \end{cases}; \tag{3}$$

in which $\dot{r} = \frac{dr}{dt}$ is the apposition or resorption rate (μm/day) (Figure 1 and Table 1). The quantities c_1, c_2, and c_3 are empirical constants that were calibrated, $c_i = \tan\theta_i$ (Figure 1); and $\pm w$ defines the dead threshold zone for the stimulus.

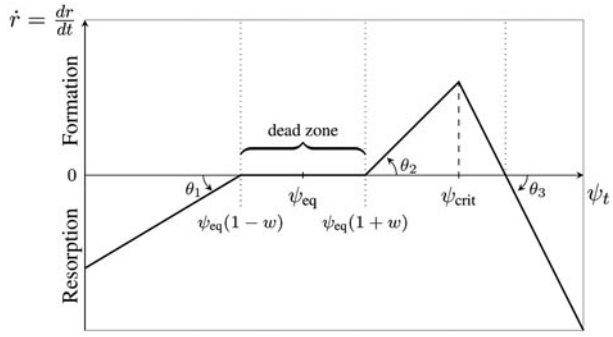

Figure 1. Bone remodeling as a function of mechanical stimulation.

Table 1. Constants used in the bone remodeling simulation.

Constants	Values (Pa)
ψ_{eq}	4.0×10^7
ψ_{crit}	1.5×10^8
w	1.0×10^7
c_1	1.0×10^{-11}
c_2	3.0×10^{-11}
c_3	1.0×10^{-11}

When equating the third and fourth terms of Equation 3 and making $\psi_t = \psi_{crit}$, the variable z represents the measure of the bone tissue damage, so one can write

$$z = -\frac{c_2}{c_3}\left[\left(\psi_{crit} - \psi_{eq}\right) - w\right]. \quad (4)$$

After determining the apposition–resorption rate (μm/day), the new density of the bone can be calculated as

$$\dot{\rho} = \dot{r} S_v \rho_t; \quad (5)$$

in which S_v is the bone surface area per unit tissue volume (4 μm^{-1}); and ρ_t is the true density of the bone tissue (2.0 g/cm^3; assumed to be equal to the density of fully mineralized tissue) (Eser et al. 2013). The maximum apparent density allowed is $\rho_{max} = 1.80$ g/cm^3, whereas the minimum apparent density is $\rho_{min} = 1.20$ g/cm^3 (Lin et al. 2009). The new density (or apparent density, ρ) of the bone can be related to the elastic modulus of the bone through the equation of Weinans (Weinans et al. 1992):

$$E = 3790\,\rho^3 \quad (6)$$

This equation can be used for both cortical and trabecular bones since bone remodeling takes place on bone surfaces of marrow spaces/voids in cancellous bone and Haversian canals in cortical bone.

The period of evaluation was set to 3, 6, and 12 months, in which 120 loading cycles corresponded to one day, or one iteration of the model. After each interaction, the new elastic modulus of bone was calculated and used for the next time step. The material properties of bone were updated (i.e. remodeled) considering the results of the previous analyses by using the programed subroutine. The code was developed by the authors by modification of the Isotropic Stanford bone remodeling model.

The bone remodeling process can be predicted mathematically (Figure 1) and all equations were coded using FORTRAN 90 and the APDL programing facility in the ANSYS software package (MSC. Marc-Mentat 2005, MSC. Software Corporation, Los Angeles, CA).

Bone remodeling simulation by 3D FEA

The right posterior region of a partially edentulous mandible with the second premolar and second molar was reproduced using Solidworks 2012, on the basis of computed tomography images. The bone model comprised the cancellous bone surrounded by a 2-mm-thick layer of cortical bone. CAD models of a 4-mm-diameter implant with an external hexagon platform and a 7-, 10-, or 13-mm height were aligned in the bone models at the first molar region. Afterward, a cemented single crown was constructed with a zirconium infrastructure and a uniform feldspathic ceramic cover layer. The cement was 50 μm in thickness, and all materials were considered homogenous, isotropic, and linearly elastic.

In the Ansys Workbench finite elements analysis (FEA) software, a mesh convergence test was performed in all models and the element edge length was varied between 3.0 and 0.6 mm. The convergence test result shows a relative error in energy norm of 5% for approximately 1000 degrees of freedom. The tetrahedron element has quadratic interpolation functions and is defined by ten nodes having three degrees of freedom at each node. The elastic moduli and Poisson's ratios of the cortical and cancellous bones were 14.95 and 1.14 GPa and 0.3 and 0.26, respectively (Cruz et al. 2009). The implant, prosthetic components, and prosthetic screws were modeled in pure titanium grade IV, defined by an elastic modulus of 110 GPa and a Poisson's ratio of 0.35 (Dittmer et al. 2010). The feldspathic ceramic cover layer in the crown had an elastic modulus of 70 GPa, whereas the zirconium infrastructure was assigned an elastic moduli of 210 GPa and Poisson ratio of 0.27 (Sotto-Maior et al. 2012).

Boundary conditions were defined by fixing the mesial and distal bone segment surfaces. The 200 N occlusal loading was distributed in five 1.5 mm² contact areas on the occlusal surface (Figure 2) of the molar crown (Sotto-Maior et al. 2012). The results of the analyses were examined at three time intervals, namely 3, 6, and 12 months.

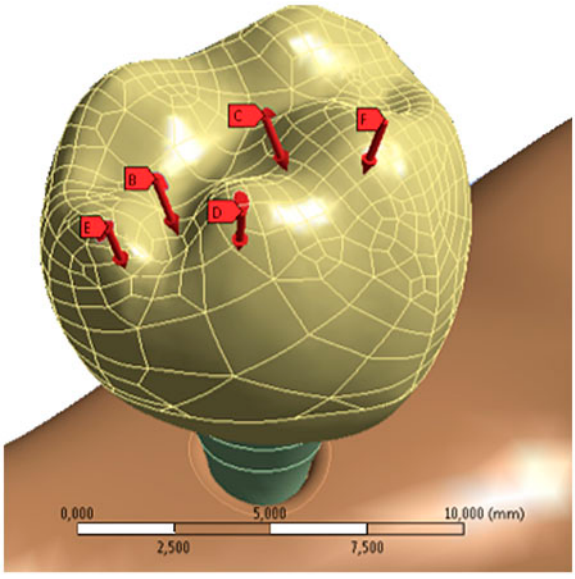

Figure 2. The occlusal load of 200 N was equally distributed on five areas of the occlusal surface of the molar crown to simulate the functional contact against the antagonist tooth.

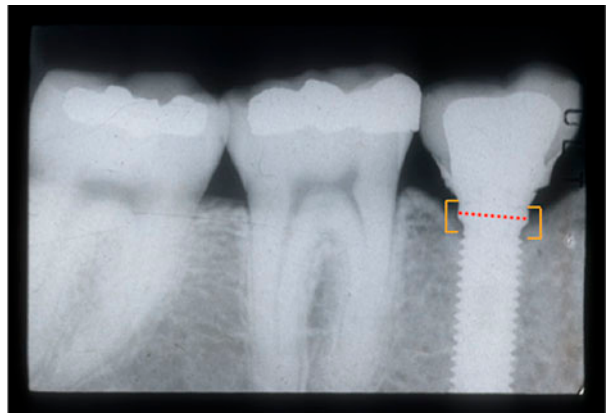

Figure 3. Bone loss measurement.
Notes: The dotted line represents the diameter of each implant (used as reference) and the yellow brackets represent the bone loss measured at the mesial and distal sides of each implant from the platform up to the first bone-to-implant contact.

Clinical model assessment/validation

The clinical section of this study was approved by Ethics Committee of the São Leopoldo Mandic Institute and Research Center. A total of 45 dental implants placed at a lower molar region (Brånemark MkIII, Nobel Biocare, CA, USA) were included in the present study. All implants had a 4.0-mm diameter and were divided according to their length: 7, 10, or 13 mm (n = 15). The inclusion criteria were as follows: subjects with good general health at the time of surgery, no signs of occlusal parafunction, no smokers or bone grafting at the surgical site, and natural or fixed opposing teeth. The implants must have been placed at least after six weeks of healing after tooth extraction and must have been positioned at the crest level.

All surgeries were performed by the same surgeon and under antibiotic and anti-inflammatory therapy. The alveolar ridge was exposed by using a full-thickness flap under local anesthesia; osteotomy was performed following the manufacturer's instructions, and implants were placed at the crestal level. After 12–16 weeks of submersed healing, the implants were loaded.

Marginal bone levels were assessed by digital periapical radiographs at resolution of 26.3 lp/mm (Snapshot; KaVo do Brasil, Joinville, SC, Brazil) using the long-cone parallel technique recorded at the day of prosthetic loading (baseline) and at the 12-month follow-up to determine bone resorption resulting from the remodeling process (Roos-Jansaker et al. 2006). Measurements were performed by a blind expert investigator using an image processing software (UTHSCSA Image Tool for Windows, University of Texas Health Science Center, San Antonio, TX, USA), in which the implant diameter of each image was used as a reference in measuring the linear distance from the implant platform level to the first bone-to-implant contact (Figure 3). The difference between the measurement at the baseline and at the 12-month follow-up determined the marginal bone resorption and it was recorded for each implant.

For the validation of the mathematical model, the clinical data of crestal bone loss were used. The prediction models were developed by means of a linear regression analysis and the differences between the predicted reduction of bone density and the observed bone resorption were expressed in terms of Studentized residuals (Cook & Weisberg 1982). The clinical data of bone loss were analyzed using one-way ANOVA, and Tukey's test was used to compare bone remodeling among the different implant lengths (SPSS version 17.0, IBM Corporation, Armonk, NY, USA). The level of significance was fixed at 5%.

Results

The prediction of bone remodeling in the marginal cortical bone at the various time points is shown in Figure 4, in which the white and red areas represent the resorbed bone tissue. Implant length did not influence the changes in peri-implant bone density, and the final bone density distributions were similar for all groups presenting similar bone remodeling around the implant neck (Figure 5). However, there was a very slight time-dependent increase on average in the values of density in the cortical bone.

Compressive stress was concentrated on the cortical bone around the first thread, independent of implant length and the remodeling process (Figure 6).

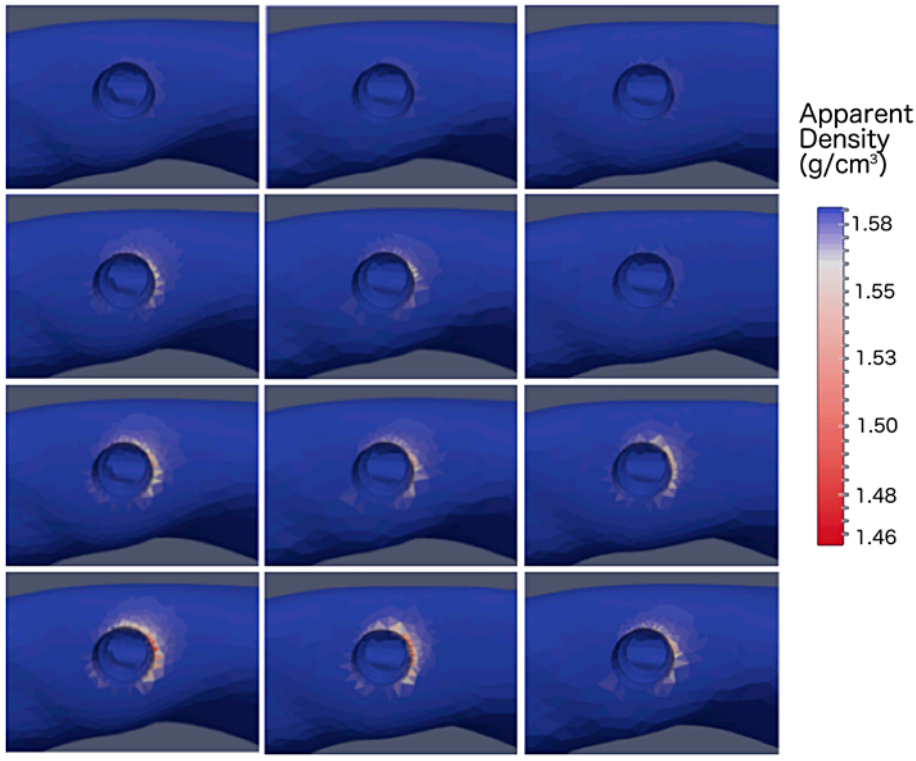

Figure 4. Bone apparent density of cortical bone around the implant neck of a 7- (left column), 10- (middle column), and 13- (right column) mm-long implant at loading (first line), 3 months (second line), 6 months (third line), and 12 months after loading (fourth line).

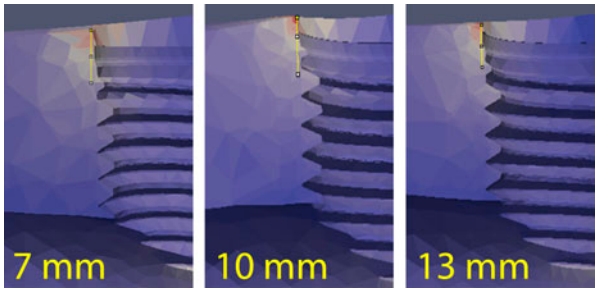

Figure 5. Simulated bone remodeling at mesial side of the 7-, 10-, and 13-mm implants after 12 months of loading.

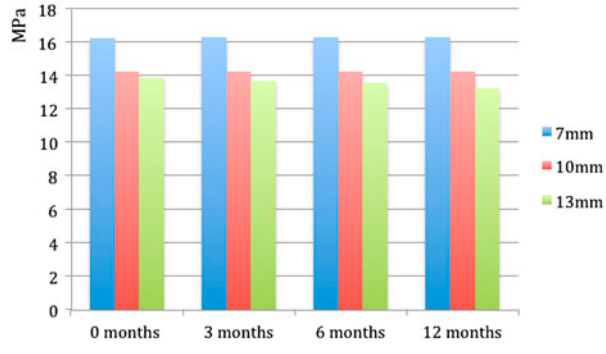

Figure 6. Compressive stress of various implant lengths evaluated at the moment of loading and 3, 6, and 12 months after loading.

Clinical data on the marginal bone remodeling were similar among all implant lengths ($p > 0.05$) and were within the same range of the mathematical predictions (Table 2). The clinical bone loss was similar from that predicted in any of the implant lengths.

Discussion

An extensive bone remodeling occurs, especially in marginal bone, around the dental implants during the first year of loading (Albrektsson et al. 1986; Türk et al. 2013). Thus, it is important to consider this physiological phenomenon in order to differentiate it from the bone loss derived from peri-implantitis situations. In the present study, the mathematical model and prospective clinical study was used to predict how bone remodels and its biomechanical consequence to dental implants of different lengths. The compressive stress and strain concentrated on the cervical portion of the peri-implant bone suggests a significant impact on the biological activity of the bone tissue at this area during the first year of loading.

Table 2. Clinical and simulated bone loss (mm) after 12 months of loading.

Implant length	Clinical bone loss (mean ± s.d.)		Simulated bone loss
	Mesial	Distal	
7 mm	1.11 ± 0.42[*, ***]	1.19 ± 0.41[****, ******]	1.25
10 mm	1.23 ± 0.39[*, **, ***]	1.41 ± 0.32[****, *****]	1.66
13 mm	1.02 ± 0.28[**, ***]	1.08 ± 0.40[*****, ******]	0.92

[*]$p = 0.218$; [**]$p = 0.940$; [***]$p = 0.966$; [****]$p = 0.845$; [*****]$p = 0.753$; [******]$p = 0.742$.

In all incidences of functional loading on the implants, the masticatory forces are transferred to the bone–implant interface through an implant-supported prosthesis. Therefore, the length of the implant may be influencing this biomechanical behavior. The results of this study corroborate with some clinical and animal studies that show a marginal bone loss around the neck of a dental implant during the first year of loading (Guljé et al. 2013; Jung et al. 1996). However, after 12 months of loading, a 7-mm-long implant showed a 22.14 and 37.57% higher compressive stress compared with the 10- and 13-mm-long implants, respectively. This outcome of shorter implants is in accordance with previous studies that used finite element analysis (Baggi et al. 2008; Vairo & Sannino 2013).

However, a 2-mm vertical resorption of the crestal bone during the first year of functional loading has been assumed as normal by the dental community (Albrektsson et al. 1986; Froum et al. 2013). Papaspyridakos et al. (2012) and Jung et al. (1996) reported a marginal bone loss in the first year of 1.5 and 1.2–2 mm, respectively, and all authors considered this as a good outcome, especially because of the expected tissue stability after this period with a bone loss lower than 0.2 mm/year at the subsequent years (Albrektsson et al. 1986). In the present study, all implants were within this threshold despite the reduction of bone density, indicating a physiological bone remodeling phenomenon. Although the 7-mm implant length showed a higher stress and strain after 12 months, the magnitude of the stress and strain may be within the limits of bone physiology (Duyck et al. 2001).

The validation assessment of a computer model is to quantify confidence in the predictive capability of the model by comparison with experimental data. In the present study, there was no statistically significant difference between the observed bone loss and the predicted bone density reduction around the different implant lengths. This observation confirms the predictive usefulness of the mechanoregulatory tissue differentiation model that describes the changes in bone density over time using an algorithm, assuming that the bone response is directly related to the loading effect in a time-dependent manner (Eser et al. 2009, 2013; Wang et al. 2013).

In general, bone remodeling can be defined as an adaptation process where bone morphology gradually changes to adapt to the environment (Mellal et al. 2004). There are two opposite scenarios that interplay during bone remodeling: bone resorption and/or deposition (Figure 1). Bone resorption occurs when the stress stimulus is below a certain limit, while formation occurs when it is above a certain limit; however, resorption occurs again in response to overload. Another scenario that takes place together with the bone remodeling is bone maturation, in which the osteocytes further the transportation of calcium and other ions from the blood plasma to the woven bone (Gong et al. 2010). Thus, overall structural changes can be an adaptive phenomenon to improve the capacity of the bone to endure biomechanical activities, causing the overall strain to drift back into the physiological state (McNamara & Prendergast 2007).

Bone requires a certain level of mechanical stimulation to maintain its physiological state, which is also known as its homeostatic condition (Cehreli & Akca 2005). Within this mechanical level, bone tissue balance is maintained by antagonistic mechanosensory pathways on osteoblasts and osteoclasts (Kokkinos et al. 2009). However, when the homeostatic condition is disturbed by loading below or above the physiological limit, bone resorption can occur. Underloading can decrease viability and increase apoptosis of osteocytes (Eser et al. 2013), whereas overloading induces microcracks in the bone, which may then cause osteocyte apoptosis (Raggatt & Partridge 2010).

Although marginal bone loss can be influenced by a number of parameters such as surgical trauma, peri-implantitis, microgap, biological width, implant crest module, flapless or flapped procedures, implant–abutment connection, prosthetic considerations, implant design, and patient's habits (Froum et al. 2013), the present study mainly focused on biomechanical factors. However, the properties and geometrics of the tissue used in FEA modeling are simplified and linear and can be considered as a limitation of the study. The input tissue properties were, however, derived from *in vivo* stiffness data and the geometric features were derived from real bone tissue tomographic data, which therefore gives us confidence on the validity of the FEA modeling. Another limitation is that the precise external loading conditions and material properties were not always known, thus simplifying the assumptions of this study.

Conclusions

The mechanoregulatory tissue differentiation model is useful in explaining the morphological changes that occur in bone in response to biomechanical loading. Although implant length influenced the stress and strain

levels on the cortical bone surrounding the implant neck, this did not affect the bone remodeling process around single dental implants during the first year of loading.

Acknowledgments

The authors would like to thank the Conselho Nacional de Desenvolvimento Científico e Tecnológico (CNPq #2011/14001-3) for the scholarship granted to the first author.

References

Adell R. 1983. Clinical results of osseointegrated implants supporting fixed prostheses in edentulous jaws. J Prosthet Dent. 50:251–254.

Albrektsson T, Zarb G, Worthington P, Eriksson AR. 1986. The long-term efficacy of currently used dental implants: a review and proposed criteria of success. Int J Oral Maxillofac Implants. 1:11–25.

Baggi L, Cappelloni I, Di Girolamo M, Maceri F, Vairo G. 2008. The influence of implant diameter and length on stress distribution of osseointegrated implants related to crestal bone geometry: a three-dimensional finite element analysis. J Prosthet Dent. 100:422–431.

Brånemark PI, Breine U, Adell R, Hansson BO, Lindström J, Ohlsson Å. 1969. Intra-osseous anchorage of dental prostheses: I. Experimental studies. Scand J Plast Reconstr Surg Hand Surg. 3:81–100.

Cehreli MC, Akca K. 2005. Mechanobiology of bone and mechanocoupling of endosseous titanium oral implants. J Long Term Eff Med Implants. 15:139–152.

Chou H-Y, Müftü S. 2013. Simulation of peri-implant bone healing due to immediate loading in dental implant treatments. J Biomech. 46:871–878.

Cook RD, Weisberg S. 1982. Residuals and influence in regression. New York (NY): Chapman and Hall.

Cruz M, Wassall T, Toledo EM, da Silva Barra LP, Cruz S. 2009. Finite element stress analysis of dental prostheses supported by straight and angled implants. Int J Oral Maxillofac Implants. 24:391–403.

Dittmer MP, Kohorst P, Borchers L, Stiesch M. 2010. Influence of the supporting structure on stress distribution in all-ceramic FPDs. Int J Prosthodont. 23:63–68.

Duyck J, Naert I, Ronold HJ, Ellingsen JE, Van Oosterwyck H, Vander Sloten J. 2001. The influence of static and dynamic loading on marginal bone reactions around osseointegrated implants: an animal experimental study. Clin Oral Implants Res. 12:207–218.

Eser A, Tonuk E, Akca K, Cehreli MC. 2009. Numeric simulation of time-dependent remodeling of bone around loaded oral implants. Int J Oral Maxillofac Implants. 24:597–608.

Eser A, Tonuk E, Akca K, Dard MM, Cehreli MC. 2013. Predicting bone remodeling around tissue- and bone-level dental implants used in reduced bone width. J Biomech. 46:2250–2257.

Frost HM. 2003. Bone's mechanostat: a 2003 update. Anat Rec A Discov Mol Cell Evol Biol. 275A:1081–1101.

Froum SJ, Rosen PS, Clem DS. 2013. Response to 'on crestal/marginal bone loss around dental implants'. Int J Periodontics Restorative Dent. 33:407–409.

Gong H, Zhu D, Gao J, Lv L, Zhang X. 2010. An adaptation model for trabecular bone at different mechanical levels. Biomed Eng Online. 9:32.

Guljé F, Abrahamsson I, Chen S, Stanford C, Zadeh H, Palmer R. 2013. Implants of 6 mm vs. 11 mm lengths in the posterior maxilla and mandible: a 1-year multicenter randomized controlled trial. Clin Oral Implants Res. 24:1325–1331.

Hof M, Pommer B, Zukic N, Vasak C, Lorenzoni M, Zechner W. 2015. Influence of prosthetic parameters on peri-implant bone resorption in the first year of loading: a multi-factorial analysis. Clin Implant Dent Relat Res. 17:e183–e191.

Huiskes R. 2000. If bone is the answer, then what is the question? J Anat. 197:145–156.

Jacobs CR, Levenston ME, Beaupré GS, Simo JC, Carter DR. 1995. Numerical instabilities in bone remodeling simulations: the advantages of a node-based finite element approach. J Biomech. 28:449–459.

Jung YC, Han CH, Lee KW. 1996. A 1-year radiographic evaluation of marginal bone around dental implants. Int J Oral Maxillofac Implants. 11:811–818.

Kokkinos PA, Zarkadis IK, Kletsas D, Deligianni DD. 2009. Effects of physiological mechanical strains on the release of growth factors and the expression of differentiation marker genes in human osteoblasts growing on Ti-6Al-4V. J Biomed Mater Res A. 90A:387–395.

Levenston ME, Beaupré GS, Jacobs CR, Carter DR. 1994. The role of loading memory in bone adaptation simulations. Bone. 15:177–186.

Lin D, Li Q, Li W, Swain M. 2009. Dental implant induced bone remodeling and associated algorithms. J Mech Behav Biomed Mater. 2:410–432.

Mahnama A, Tafazzoli-Shadpour M, Geramipanah F, Mehdi Dehghan M. 2013. Verification of the mechanostat theory in mandible remodeling after tooth extraction: animal study and numerical modeling. J Mech Behav Biomed Mater. 20:354–362.

McNamara LM, Prendergast PJ. 2007. Bone remodelling algorithms incorporating both strain and microdamage stimuli. J Biomech. 40:1381–1391.

Mellal A, Wiskott HWA, Botsis J, Scherrer SS, Belser UC. 2004. Stimulating effect of implant loading on surrounding bone. Clin Oral Implants Res. 15:239–248.

Monje A, Suarez F, Galindo-Moreno P, García-Nogales A, Fu J-H, Wang H-L. 2014. A systematic review on marginal bone loss around short dental implants (<10 mm) for implant-supported fixed prostheses. Clin Oral Implants Res. 25:1119–1124.

Papaspyridakos P, Chen C-J, Singh M, Weber H-P, Gallucci GO. 2012. Success criteria in implant dentistry: a systematic review. J Dent Res. 91:242–248.

Qian J, Wennerberg A, Albrektsson T. 2012. Reasons for marginal bone loss around oral implants. Clin Implant Dent Relat Res. 14:792–807.

Raggatt LJ, Partridge NC. 2010. Cellular and molecular mechanisms of bone remodeling. J Biol Chem. 285:25103–25108.

Roos-Jansaker AM, Lindahl C, Renvert H, Renvert S. 2006. Nine- to fourteen-year follow-up of implant treatment. Part II: presence of peri-implant lesions. J Clin Periodontol. 33:290–295.

Schulte FA, Lambers FM, Webster DJ, Kuhn G, Müller RG. 2011. *In vivo* validation of a computational bone adaptation model using open-loop control and time-lapsed micro-computed tomography. Bone. 49:1166–1172.

Shunmugasamy VC, Gupta N, Coelho PG. 2010. High strain rate response of rabbit femur bones. J Biomech. 43:3044–3050.

Sotto-Maior BS, Senna PM, da Silva WJ, Rocha EP, Del Bel Cury AA. 2012. Influence of crown-to-implant ratio, retention system, restorative material, and occlusal loading on stress concentrations in single short implants. Int J Oral Maxillofac Implants. 27:e13–e18.

Stanford CM, Brand RA. 1999. Toward an understanding of implant occlusion and strain adaptive bone modeling and remodeling. J Prosthet Dent. 81:553–561.

Türk AG1, Ulusoy M, Toksavul S, Güneri P, Koca H. 2013. Marginal bone loss of two implant systems with three different superstructure materials: a randomised clinical trial. J Oral Rehabil. 40:457–463.

Vairo G, Sannino G. 2013. Comparative evaluation of osseointegrated dental implants based on platform-switching concept: influence of diameter, length, thread shape, and in-bone positioning depth on stress-based performance. Comput Math Methods Med. 25:1–15.

Wang C, Li Q, McClean C, Fan Y. 2013. Numerical simulation of dental bone remodeling induced by implant-supported fixed partial denture with or without cantilever extension. Int J Numer Method Biomed Eng. 29: 1134–1147.

Wazen RM, Currey JA, Guo H, Brunski JB, Helms JA, Nanci A. 2013. Micromotion-induced strain fields influence early stages of repair at bone–implant interfaces. Acta Biomater. 9:6663–6674.

Weinans H, Huiskes R, Grootenboer HJ. 1992. The behavior of adaptive bone-remodeling simulation models. J Biomech. 25:1425–1441.

Woda A, Mishellany A, Peyron M. 2006. The regulation of masticatory function and food bolus formation. J Oral Rehabil. 33:840–849.